# Imaging Mimics of Brain Tumors

Joseph H. Donahue, MD[a], Sohil H. Patel, MD[a], Camilo E. Fadul, MD[b], Sugoto Mukherjee, MD[a,*]

**KEYWORDS**

• Brain tumor • Central nervous system neoplasm • Tumor mimic • Tumefactive demyelination

**KEY POINTS**

- Tumor mimics may account for 4% to 13% of referrals to a neuro-oncology service, so consideration of nonneoplastic processes is critical during initial evaluation of CNS neoplasia.
- Leveraging specific imaging signs and advanced imaging techniques detailed herein may add diagnostic confidence when considering various autoimmune, infectious, and vascular tumor mimics.
- Variability in ancillary laboratory diagnostics, including serologic and various immunohistochemical tests, may confer sufficiently low negative predictive values such that tumor mimics may still be considered on a clinical and imaging basis despite an unrevealing laboratory evaluation.

## INTRODUCTION

Although most patients referred to neuro-oncology with the suspicion of brain tumor by imaging harbor a neoplasm, in some cases the abnormality has a nonneoplastic cause. A wide variety of nonneoplastic entities may closely resemble the imaging findings of primary or metastatic intracranial neoplasia, posing diagnostic challenges for the referring provider and the radiologist. Autoimmune, infectious, and vascular diseases have particular potential for misdiagnosis as brain tumors given the often nonspecific neurologic symptoms and ambiguous imaging features.[1–3] These "tumor mimics" may account for 4% to 13% of patient referrals to neuro-oncology; and when imaging is ordered by neuro-oncologists with the presumptive diagnosis of "brain tumor," it may foster a framing bias that leads the radiologist to misinterpretation of the examination.[4,5] Advances in neuroimaging quality and availability, which have increased the detection of "incidentalomas" (approximately 3% of MR imaging brain scans), potentiates the possibility for such referrals to neuro-oncologists or neurosurgeons.[6–8] The consequences of an incorrect imaging diagnosis of intracranial neoplasia are obvious, with unnecessary surgical procedures and misdirected medical therapies yielding a likelihood of patient harm and legal liability.

In this article, we provide a framework for the radiologist to identify "brain tumor mimics" by highlighting imaging and laboratory pearls and pitfalls, and illustrating unique and frequently encountered lesions. Because the initial imaging in most patients with these lesions follows a generic brain MR imaging protocol dictated by institutional practice, we describe features of the various tumor mimics on common MR imaging brain sequences that are applicable to routine clinical imaging studies.

## IMAGING FINDINGS

### *Demyelinating and Inflammatory Disorders*

Although multiple sclerosis typically displays small multifocal perivenular demyelinating plaques with a propensity for the callososeptal interface that disseminate in space and time, larger tumefactive lesions may occasionally constitute the imaging

[a] Department of Radiology and Medical Imaging, University of Virginia Health System, PO Box 800170, Charlottesville, VA 22908-0170, USA; [b] Department of Neurology, University of Virginia Health System, PO Box 800432, Charlottesville, VA 22908-0170, USA
* Corresponding author.
*E-mail address:* sm5qd@virginia.edu

Radiol Clin N Am 59 (2021) 457–470
https://doi.org/10.1016/j.rcl.2021.02.003

presentation. In such cases, almost one-third of the larger tumefactive lesions can be the only lesion, potentially leading to misdiagnosis as neoplasia. Solitary and/or tumefactive lesions are more likely to occur in the uncommon multiple sclerosis variants of Marburg and Schilder diseases.[9]

The tumefactive demyelinating lesions can have local mass effect and edema (although disproportionally less when compared with tumors of the same size), centered within the deep white matter in the supratentorial cortex. Other imaging features include computed tomography (CT) hypoattenuation and T2 hypointense rim.[10] When these demonstrate enhancement, it is classically in the form of an incomplete ring, with the incomplete segment of the ring facing the cortex.[11] The enhancing segment represents the leading edge of demyelination, facing the white matter side of the lesion. Dilated veins have been seen within the central part of these lesions, and may be well demonstrated on susceptibility-weighted imagining (SWI). Usually these lesions demonstrate increased diffusivity, with decreased perfusion and nonspecific MR spectroscopy findings (with elevated choline, decreased N-acetylaspartate (NAA), and high lactate) when compared with lymphomas.[12] A rapid response to steroid helps in narrowing the diagnosis.

Acute disseminated encephalomyelitis (ADEM) is a unique autoimmune-mediated demyelinating disease, initiated by an infection (or immunization), which leads to myelin antibodies. Imaging usually reveals multifocal subcortical and periventricular lesions, with involvement of the basal ganglia, posterior fossa, and cranial nerves. Many of the white matter lesions have ill-defined "cotton-ball" like appearance on T2 and FLAIR series with a varied enhancing appearance ranging from linear, punctate, to partial/incomplete ring like enhancement for some of the larger lesions.[13] Larger "tumefactive" lesions when present appear similar to those seen in multiple sclerosis (**Fig. 1**). In cases of acute hemorrhagic leukoencephalitis, microhemorrhages or macrohemorrhages are most evident on SWI sequences,[14] occasionally resembling hemorrhagic neoplasms.

Neuromyelitis optica and neuromyelitis optica spectrum disorder (NMOSD) are autoimmune-mediated demyelinating disorders because of antibodies against aquaporin-4. Neuromyelitis optica–IgG is a specific biomarker that is present in most of these patients. The brain lesions in NMOSD involve the brainstem, hypothalamus, and other periventricular areas, and unlike tumefactive demyelinating lesions, it is unlikely for them to be mistaken for tumors.[15] In rare cases, tumefactive demyelinating lesions is seen in neuromyelitis optica or NMOSD, with similar imaging features as discussed previously. It is more likely for the long segment cord lesions to be mistaken for a spinal cord tumor if there is lack of intracranial or optic nerve involvement.

Myelin oligodendrocyte glycoprotein (MOG) is a cellular adhesion molecule expressed on the cell surface of oligodendrocytes and myelin sheaths within the central nervous system (CNS). Clinical presentation is strongly influenced by age and correlates generally with imaging phenotypes. The usual imaging patterns of presentation include a leukodystrophy-like pattern, an ADEM-like pattern, and an NMOSD-like pattern. However, they can rarely present on imaging as a demyelinating pseudotumor with imaging findings similar to a tumefactive demyelinating lesion detailed previously.[16]

## Neurosarcoid

Sarcoidosis is a complex multisystem granulomatous disease that is believed to have an autoimmune origin.[17] Although the most commonly involved organ is the lung, extrapulmonary sarcoidosis frequently occurs, with CNS involvement present in 10% to 20% of patients. Many patients with neurosarcoidosis remain asymptomatic, with only 5% demonstrating significant imaging findings, including possible involvement of the brain, blood vessels, spinal cord, dura, optic nerves, bones, and the adjacent soft tissues in the head and neck.

Neurosarcoidosis can mimic brain tumors in multiple different ways.[18] Large dural-based masses can mimic meningiomas, whereas nodular enhancing lesions along cranial nerves is characterized as schwannomas or neurofibromas. Involvement of choroid plexuses can mimic enhancing intraventricular tumors. Although the parenchymal involvement in neurosarcoidosis is frequently along perivascular spaces, causing a vasculitic-like picture, larger coalescing granulomas within the brain can present as expansile tumefactive lesions with local mass effect and edema (**Fig. 2**).[19] Unless the neuroradiologist is cognizant of this entity, these lesions are misdiagnosed as lymphoma or idiopathic inflammatory pseudotumor. Rarely, there is need for a biopsy to demonstrate the noncaseating granulomas, multinucleated giant cells, epithelioid histiocytes, and benign lymphocytes and plasma cells characteristic of this entity.

## Autoimmune Encephalitis

Autoimmune encephalitis represents a challenging set of diagnoses with varied clinical presentations.

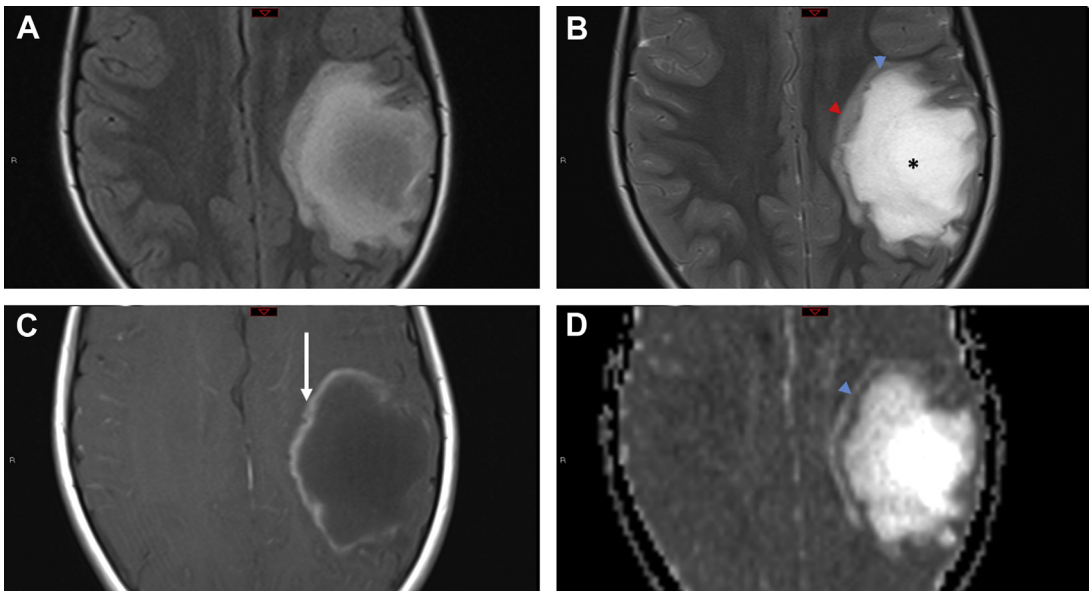


**Fig. 1.** Tumefactive demyelinating lesion in ADEM. Axial FLAIR (*A*), axial T2-weighted (*B*), axial postcontrast T1-weighted (*C*), and axial apparent diffusion coefficient (ADC) map (*D*) MR images in an 8 year old with complaints of foot numbness and progressive clumsiness determined to have ADEM. The leading edge of demyelination is characterized by the incomplete rim enhancement (*white arrow* in *C*) with corresponding thin linear T2 and ADC hypointensity (*blue arrowheads* in *B* and *D*, respectively). The T2 images show a characteristic "zoned" appearance with the central lesion showing marked hyperintensity (*asterisk* in *B*), which is marginated by the leading edge of demyelination (*blue arrowhead* in *B*) that separates the central lesion from a rim of perilesional edema (*red arrowhead* in *B*).

In most cases, specific antibodies directed against CNS cells are found in peripheral blood or cerebrospinal fluid (CSF). Although autoimmune encephalitis has been grouped according to the antibodies recognized epitope (intracellular vs cellular surface) and if the antibodies are mechanistically responsible for the disease or an epiphenomenon, the MR imaging findings are indistinguishable between these two groups. The most common imaging appearance is the involvement of the limbic system, which manifests as either unilateral or bilateral involvement of mesial temporal lobes and thalami/basal ganglia with patchy enhancement.[20] Nevertheless, the imaging abnormalities may occur in other cerebral lobes. Rarely, these lesions exhibit swelling and edema that can mimic infiltrative gliomas.

### *TREX1-Associated Retinal Vasculopathy with Cerebral Leukodystrophy*

TREX1 gene–related mutations causing retinal vasculopathy and cerebral leukodystrophy are rare autosomal-dominant disorders secondary to underlying frameshift mutations that encode for major DNA exonucleases.[21] The mutations result in accumulation of abnormal DNA and RNA within cells, which are then mistakenly targeted by the host immune cells with devastating consequences. Most of these patients are middle aged, present with vision and neurologic symptoms, and have a positive family history.

The most common imaging findings include hyperintense white matter lesions on T2/FLAIR with near complete sparing of the gray matter. Lesions, which are usually supratentorial, may demonstrate nodular enhancement with restricted diffusion or larger mass-like lesions with irregular rim enhancement and extensive surrounding edema (**Fig. 3**). After immunosuppressive treatment, the lesions can transiently decrease in size with newer lesions appearing at different sites, giving the appearance of a migratory tumefactive process.[22]

### *Central Nervous System Infection Tumor Mimics*

#### *Pyogenic infections*

Cerebral abscesses are occasionally difficult to distinguish from neoplasm, particularly metastatic disease, because both may appear as disseminated ring-enhancing lesions localizing to the gray-white matter interface. In a series of 221 ring-enhancing lesions, Schwartz and colleagues[23] found that although neoplasia (primary

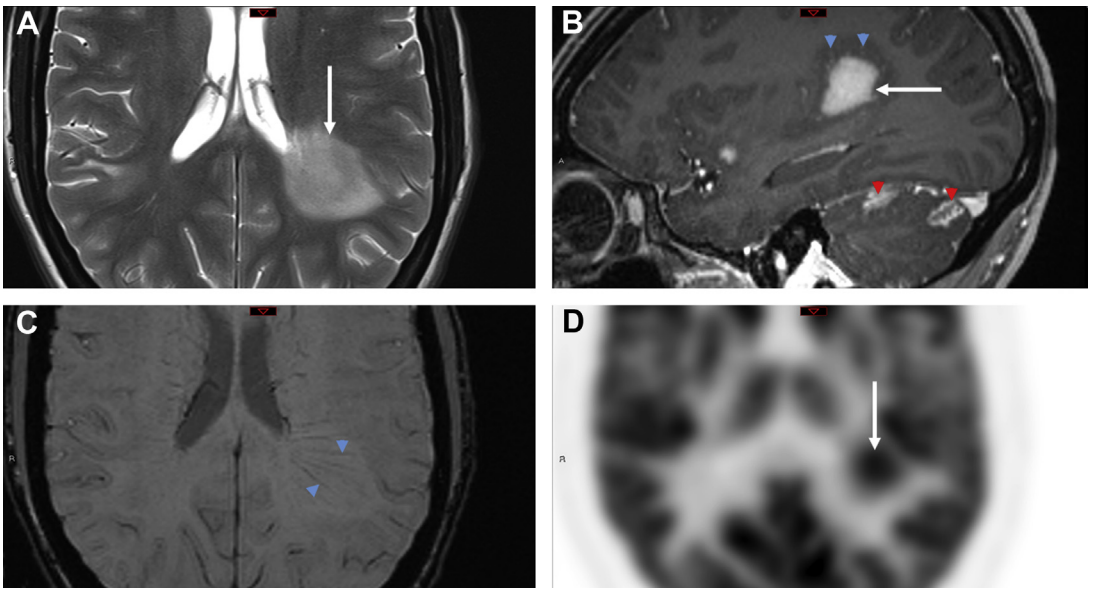


**Fig. 2.** Neurosarcoidosis. Axial T2-weighted MR image (*A*), sagittal T1-weighted postcontrast MR image (*B*), axial SWI MR image (*C*), and axial fluorodeoxyglucose PET image (*D*) in a 23 year old presenting with multiple subacute focal neurologic deficits. A mass-like area of left periatrial signal abnormality demonstrates slightly mixed intermediate/high T2 signal (*white arrow* in *A*) with corresponding homogeneous enhancement (*white arrow* in *B*). Note that the medullary veins maintain a straight course through the lesion and demonstrate slight engorgement on SWI and postcontrast series (*blue arrowheads* in *B* and *C*). Additional areas of cerebellar folia parenchymal and leptomeningeal enhancement are present (*red arrowheads* in *B*). Fluorodeoxyglucose PET images show radiotracer accumulation within the periatrial lesion (*white arrow* in *D*), measuring an average and maximum standardized uptake value of 9.2 and 12.9, respectively.

and metastatic) accounted for 72% of cases, pyogenic abscess and atypical infections accounted for 8% and 4%, respectively. In a similar investigation by Kim and colleagues,[24] concordant findings were reported, with 4% pyogenic abscess and 2.6% atypical infections.

Although metastasis are the more common underlying cause of ring-enhancing lesions, some imaging features should prompt consideration of an infectious tumor mimic. The SWI dual rim sign displays a hypointense outer rim posited to represent the fibrocollagenous abscess capsule surrounding a hyperintense inner rim thought to correspond to a zone of granulation tissue between the necrotic core and the capsule. In a study of 32 brain masses, the dual rim sign was present in 9 of 12 abscesses and 0 of 20 glioblastomas, conferring a sensitivity of 75% and a specificity of 100%.[25]

Restricted diffusion of cavity contents, one of the best known imaging features of pyogenic abscesses, is caused by the highly viscous nature of the proteinaceous exudate admixed with viable bacteria, inflammatory cells, and debris (**Fig. 4**). A meta-analysis of 11 studies found a pooled sensitivity and specificity of 95% and 94%, respectively, for the use of diffusion-weighted images (DWI) to distinguish abscess from other cerebral ring-enhancing lesions.[26] However, some pyogenic abscesses (~4%), atypical infections, or pyogenic abscesses imaged after initiation of antibiotic therapy or in an immunocompromised host may not show diffusion restriction.[27,28]

## Atypical Infections

### Toxoplasmosis

*Toxoplasma gondii* is a ubiquitous protozoan parasite prone to cause opportunistic cerebral infection, typically reactivation of latent infection, in the setting of severe immunosuppression (CD4 <100 cells/μL). Differentiating cerebral toxoplasmosis from primary CNS lymphoma (PCNSL) is often challenging on a clinical, laboratory, and imaging basis. Although there is considerable overlap of imaging, PCNSL is statistically the more likely cause in immunocompromised patients with a solitary parenchymal mass, particularly one demonstrating subependymal spread of disease, whereas toxoplasmosis is more likely multifocal with basal ganglia predilection. Both "eccentric" and "concentric" target signs favor toxoplasmosis. The eccentric target sign, present in less than 30% of cases, is recognized on postcontrast MR imaging series as a ring-enhancing lesion

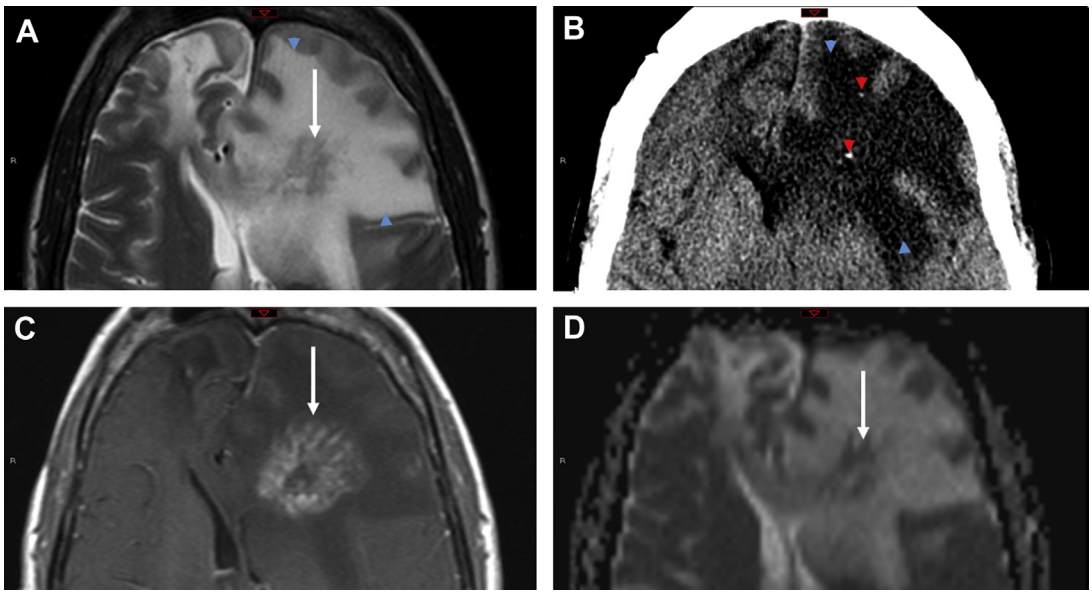


**Fig. 3.** TREX1-associated retinal vasculopathy with cerebral leukodystrophy. Axial T2-weighted MR image, axial noncontrast CT scan, axial postcontrast T1-weighted image, and axial ADC map MR image in a 45 year old presenting with headache and weakness. Extensive left frontal vasogenic edema (*blue arrowheads* in *A* and *B*) surrounds an irregular mass-like area of periventricular enhancement (*white arrow* in *C*) with corresponding intermediate signal on T2 and ADC series (*white arrows* in *A* and *D*, respectively). A few punctate foci of calcification are displayed on CT images (*red arrowheads* in *B*). A nearly identical lesion was previously present in the right frontal lobe (not shown) with biopsy revealing subacute infarction with extensive gliosis and nonspecific vasculopathy.

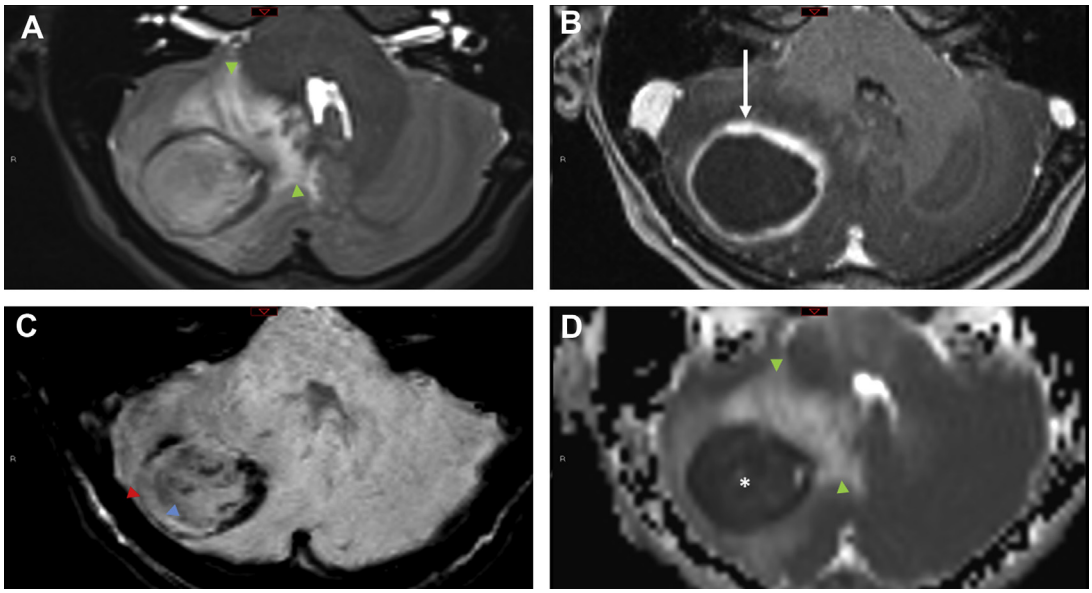


**Fig. 4.** Pyogenic abscess. Axial T2-weighted (*A*), axial postcontrast T1-weighted (*B*), axial SWI (*C*), and axial ADC map (*D*) MR images in a 10 year old presenting with headache. Vasogenic edema (*green arrowheads* in *A* and *D*) surrounds the smoothly rim-enhancing right cerebellar mass (*white arrow* in *B*). A partial dual rim sign is displayed on SWI as an inner hyperintense rim and an outer hypointense rim (*blue* and *red arrowheads* in *C*, respectively). The central abscess cavity shows nearly homogeneous diffusion restriction as low signal intensity on ADC (*asterisk* in *D*).

with a small nodular focus of enhancement along the lesion wall. The concentric target sign is shown on T2-weighted images as alternating zones of hypointensity/hyperintensity and is believed to be a more specific imaging feature (Fig. 5).[29]

Cerebral toxoplasmosis may demonstrate lower perfusion indices (regional cerebral blood volume <1.3–1.5 × normal white matter) and higher diffusion coefficient (apparent diffusion coefficient >1.6 normal white matter) than PCNSL.[30–32] By MR spectroscopy, cerebral toxoplasmosis and PCSNL may both demonstrate lipid/lactate peaks, with toxoplasmosis generally showing a suppression of other metabolite peaks and PCNSL potentially showing a prominent choline peak. The specificity of MR spectroscopy for differentiating PCNSL from other diagnoses in immunocompromised patients ranges from 27% to 83%.[33]

### *Neurocysticercosis*

The cestode *Taenia solium* (pork tapeworm) causes cysticercosis, a globally common parasitic infection in which humans act as the intermediate dead-end host. The parasitic embryos disseminate hematogenously and commonly deposit within skeletal muscle, the globes, and neural tissues, where the cysticerci then evolve through four stages of disease: vesicular, colloidal vesicular, granular nodular, and nodular calcified. Neurocysticercosis may occasionally masquerade as CNS neoplasia, particularly in the colloidal vesicular or granular nodular stages of intraparenchymal disease when rim enhancement and perilesional edema may be present. The racemose disease form, infection of the subarachnoid space, may also mimic intraventricular or suprasellar neoplasia, such as craniopharyngioma.

If present, larvae in various life stages or of varying compartmental distribution are an important feature in recognizing neurocysticercosis. For instance, the co-occurrence of parenchymal ring-enhancing lesions with calcified parenchymal or craniofacial soft tissue foci may be present. Identification of the parasitic scolex in the vesicular and colloidal vesicular stages adds certainty to the diagnosis. Typically, the scolex appears as a DWI and/or T1 hyperintense eccentric nodule or comma-shaped structure within the larger cyst (Fig. 6). DWI hyperintensity of the cysts may occur during evolution to the granular nodular phase when the fluid contents becomes more viscous.

## *Imaging Features Suggesting a Vascular Tumor Mimic*

### *Aneurysm*

Most intracranial aneurysms are acquired "true" aneurysms that arise at the branch points of major intracranial arteries, and are caused by

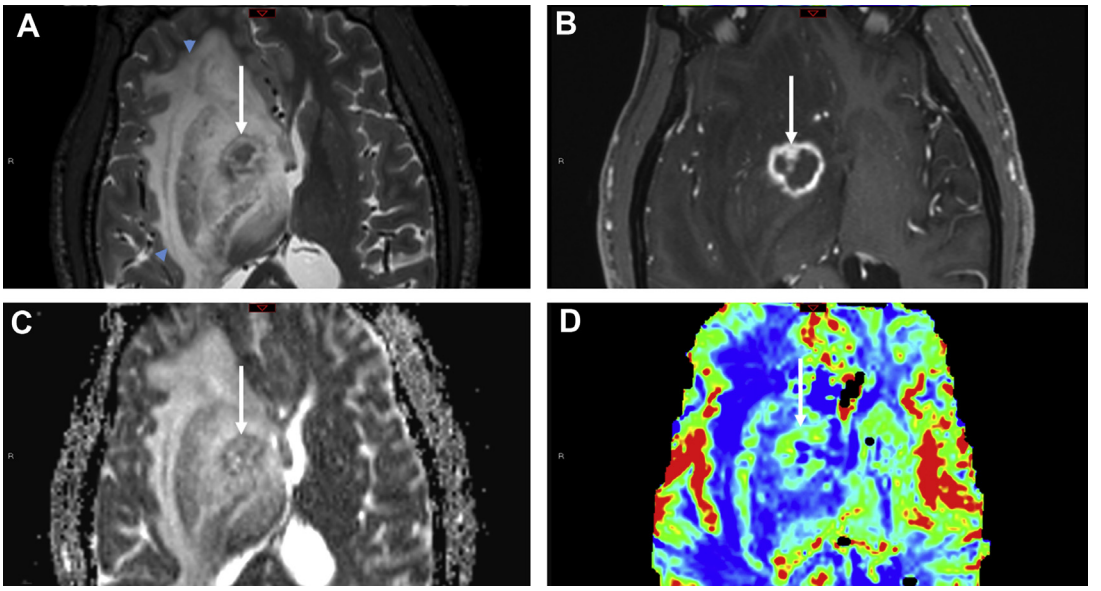


Fig. 5. Toxoplasmosis. Axial T2-weighted (*A*), axial postcontrast T1-weighted (*B*), ADC map (*C*), and axial perfusion-weighted (PWI) cerebral blood volume map (*D*) MR images in a 47-year-old immunocompromised patient presenting with headache. Right basal ganglia lesion shows the "concentric target sign" on T2-weighted images as alternating zones of hypointensity/hyperintensity (*white arrow* in *A*) and substantial perilesional vasogenic edema (*blue arrowheads* in *A*). T1-weighted images show the "eccentric target sign" as a small nodular focus of enhancement along the lesion wall (*white arrow* in *B*). The lesion shows predominantly intralesional T2 shine through on ADC map (*white arrow* in *C*) and mild capsular hyperperfusion on PWI (*white arrow* in *D*).

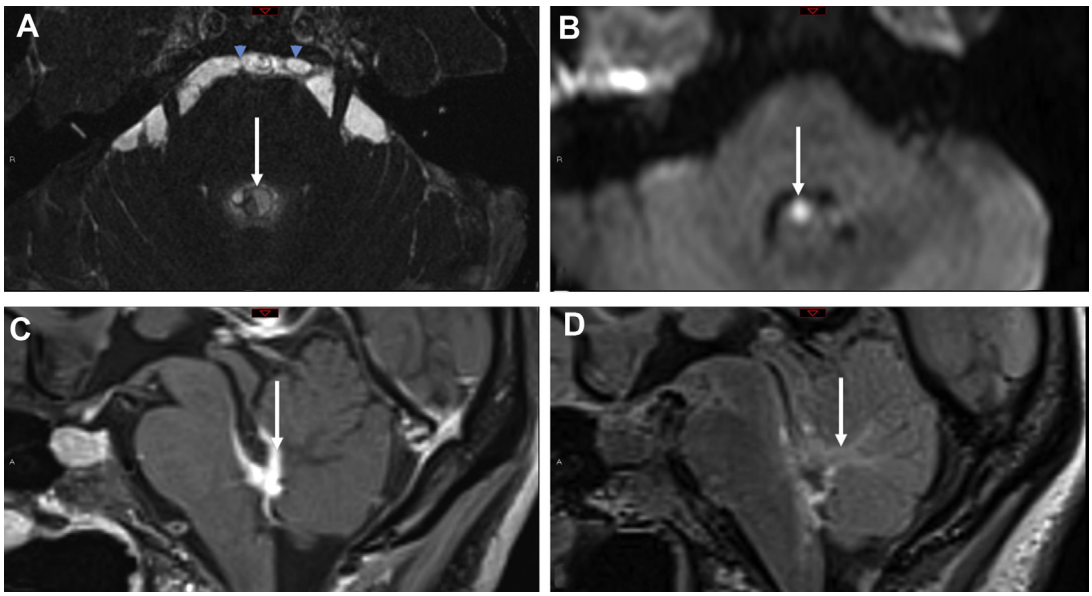


**Fig. 6.** Neurocysticercosis. Axial heavily T2-weighted (*A*), axial diffusion-weighted (*B*), sagittal T1-weighted post-contrast (*C*), and sagittal FLAIR (*D*) MR imaging in a 30-year-old patient with headache. The scolex is identifiable as a cystic intraventricular focus with corresponding diffusion restriction (*white arrows* in *A* and *B*). Inflammatory ependymal enhancement (*white arrow* in *C*) and periventricular edema (*white arrow D*) contribute to obstruction of the fourth ventricular outflow foramina and hydrocephalus (not shown). Additional racemose disease is appreciable in the prepontine cistern on heavily T2-weighted images (*blue arrowheads* in *A*).

hemodynamic stresses that are potentiated by various environmental (smoking, hypertension, alcohol abuse) and genetic factors.[34] "False" aneurysms, or pseudoaneurysms, involve complete arterial wall disruption with a specific cause, such as trauma or infection, and are variably contained by hemorrhage, clot, and fibrin, and are therefore at high risk of rupture.

On angiographic examinations (CT angiography, MR angiography), most intracranial aneurysms are easily diagnosed, appearing as rounded/saccular outpouchings that arise from branch points of the major cerebral arteries. However, aneurysms can have atypical appearances or be initially detected on nonangiographic studies, which can create diagnostic uncertainty. In particular, giant intracranial aneurysms (>2.5 cm) frequently contain mural thrombus of variable and heterogeneous signal intensity on T1- and T2-weighted imaging, an appearance that might mimic a complex, hemorrhagic neoplasm.[35] Giant aneurysms may cause local brain parenchymal mass effect and edema, similar to extra-axial neoplasms. The contrast enhancement of an aneurysm lumen can be mistaken for the avid contrast enhancement of a vascularized neoplasm. Furthermore, the location of an aneurysm may cause diagnostic confusion depending on the context. Cavernous internal carotid aneurysms might be mistaken for cavernous sinus neoplasms (eg, schwannoma, meningioma, pituitary macroadenoma). Fusiform aneurysms of the petrous internal carotid artery might be mistaken for petrous apex masses, such as cholesterol granuloma, mucocele, dermoid, or epidermoid.[36]

Several diagnostic clues may aid in the accurate identification of an intracranial aneurysm that mimics a neoplasm. On CT, aneurysms appear as rounded masses with attenuation values similar to neighboring vessels. Peripheral calcification may be present. On MR imaging, T2-weighted imaging frequently shows marked hypointense signal ("flow void") in the aneurysm lumen, although the signal intensity may vary depending on flow turbulence. Pulsation artifact in the phase encoding direction is an extremely useful sign, but not always present. Aneurysm wall thrombus commonly demonstrates "blooming" on T2*/SWI; T1 shortening; and a concentric, lamellated pattern. Contrast-enhanced three-dimensional gradient echo T1-weighted sequences (eg, MPRAGE, VIBE, BRAVO) are particularly useful for visualizing the artery from which the aneurysms arises. On such sequences, the degree of contrast enhancement of the aneurysm lumen usually matches that of the surrounding vasculature (**Fig. 7**). When aneurysm is suspected, CT angiography and MR angiography should be pursued for confirmation, with

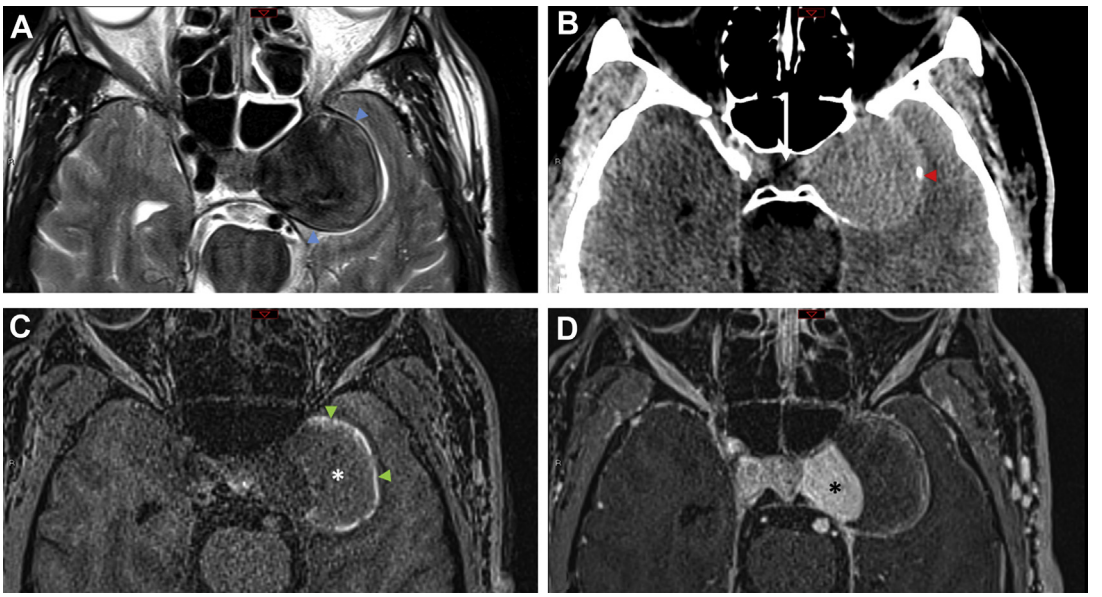


**Fig. 7.** Giant aneurysm. Axial T2-weighted MR image (*A*), axial noncontrast CT (*B*), axial noncontrast T1-weighted MR image (*C*), and axial postcontrast T1-weighted MR image (*D*) in a 63 year old presenting with left cranial nerve III palsy. The left cavernous carotid artery aneurysm wall demonstrates smooth low signal intensity on T2-weighted images (*blue arrowheads* in *A*) and peripheral calcification (*red arrowhead* in *B*). The patent portion of the aneurysm sac shows avid contrast enhancement, which approximates that of other vascular structures (*asterisk* in *D*). The nonenhancing mural thrombus within the aneurysm sac shows variable signal, with discontinuous peripheral hyperintensity (*green arrowheads* in *C*) and vague central hypointensity (*asterisk* in *C*) on T1-weighted images.

the authors generally preferring high-quality CT angiography for this purpose. On time-of-flight MR angiography, the hyperintense signal of mural thrombus caused by T1-shortening can mimic flow-related signal. Conversely, turbulent or slow blood flow through the aneurysm lumen may result in reduced flow-related signal.[37]

### *Subacute arterial infarction*

Subacute arterial cerebral infarctions (generally considered 2 days to 2 weeks following the ischemic event) mimic many of the imaging features of neoplasm. Mass effect from edema and heightened risk for hemorrhage occur during the subacute phase. DWI is variable at this stage, reflecting a combination of cytotoxic and vasogenic edema. Subacute infarctions often show contrast enhancement, reflecting endothelial damage and ingrowth of vessels with "leaky" blood-brain barriers. "Luxury" perfusion, representing infarct-bed hyperemia after arterial recanalization, shows increased cerebral blood flow on perfusion-weighted imaging.[38]

Nonetheless, there are several clues to the diagnosis of a subacute infarction. A history of acute symptom onset suggests ischemic stroke. Parenchymal injury is often restricted to a single arterial territory. The pattern of contrast enhancement is usually gyriform for cortical infarctions, or may isolate to the deep gray structures. Angiographic imaging can identify an occluded artery in the territory of the infarction. MR spectroscopy shows reduction in NAA from neuronal damage, a lactate peak, and lack of significant Cho elevation.[39] Short-term follow-up neuroimaging usually clarifies the diagnosis.

### *Venous infarction*

Venous infarctions result from venous sinus or cortical vein thrombosis. Predisposing conditions include various hypercoagulable diseases, oral contraceptive use, pregnancy, dehydration, underlying infection, neoplasm, and trauma. The clinical presentation of venous infarctions is more variable than for arterial infarctions, with symptoms that include headache, seizure, nausea and vomiting, focal neurologic deficits, and altered mental status.

Neuroimaging features include parenchymal hemorrhage, mixed vasogenic and cytotoxic edema, and mass effect.[40] The appearance of hemorrhage is variable, but may show a lobar or petechial gyriform pattern. The location of venous infarctions is an important clue to their cause

because they follow the territory drained by the thrombosed vein. For instance, thrombosis of the internal cerebral veins can cause bilateral thalamic venous ischemia.

An important step in confirming a diagnosis of venous infarction is identifying the thrombosed venous sinus or cortical vein, best displayed on MR or CT venography. Note that lack of flow void on T2 and FLAIR-weighted imaging should be interpreted with caution, and can result from turbulent and slow flow in a patient venous structure.[41]

### *Low-flow cerebral vascular malformations*

Cerebral cavernous malformations (CCMs) are slow-flow venous malformations composed of clustered thin-walled capillaries and thin fibrous adventitia, surrounded by hemosiderin and gliosis. Although most are sporadic and solitary, familial CCM syndrome or prior radiation therapy may result in multiple intracranial CCMs.[42] Although most are asymptomatic, hemorrhage into a CCM can result in headache, seizures, or focal neurologic deficit. On CT, CCMs are typically hyperdense and some show calcification. MR imaging shows a characteristic "popcorn" morphology, with regions of hypointense/hyperintense signal on T1- and T2-weighted imaging, often with a hypointense rim. T2*/SWI shows marked susceptibility blooming (**Fig. 8**). There is mild or no contrast enhancement. Recent hemorrhage of a cavernous malformation associates with acute/subacute blood products, blood-fluid levels, and adjacent brain edema. CCMs may mimic neoplasms if they are large and/or recently hemorrhaged. An important clue is the presence of a neighboring developmental venous anomaly, which frequently co-occur with CCMs.[43] In familial CCM syndrome, the presence of multiple CCMs may suggest a differential diagnosis of metastases. In this situation, most of the CCMs should neither enhance nor cause local edema, allowing for differentiation from metastasis.

Capillary telangiectasias are benign low-flow malformations composed of dilated capillaries with normal intervening brain parenchyma, usually discovered incidentally on neuroimaging. Most occur in the pons, with a minority occurring in the cerebellum and basal ganglia.[44] Capillary telangiectasias are asymptomatic lesions discovered incidentally on neuroimaging. They show subtle if any signal alteration on T1- and T2-weighted imaging. T2*/SWI shows low signal "blooming" from slow-flowing deoxyhemoglobin (**Fig. 9**). They show contrast enhancement, which, in our experience, most frequency causes a diagnostic dilemma when a patient is undergoing MR imaging to evaluate for brain metastases. Lack of edema

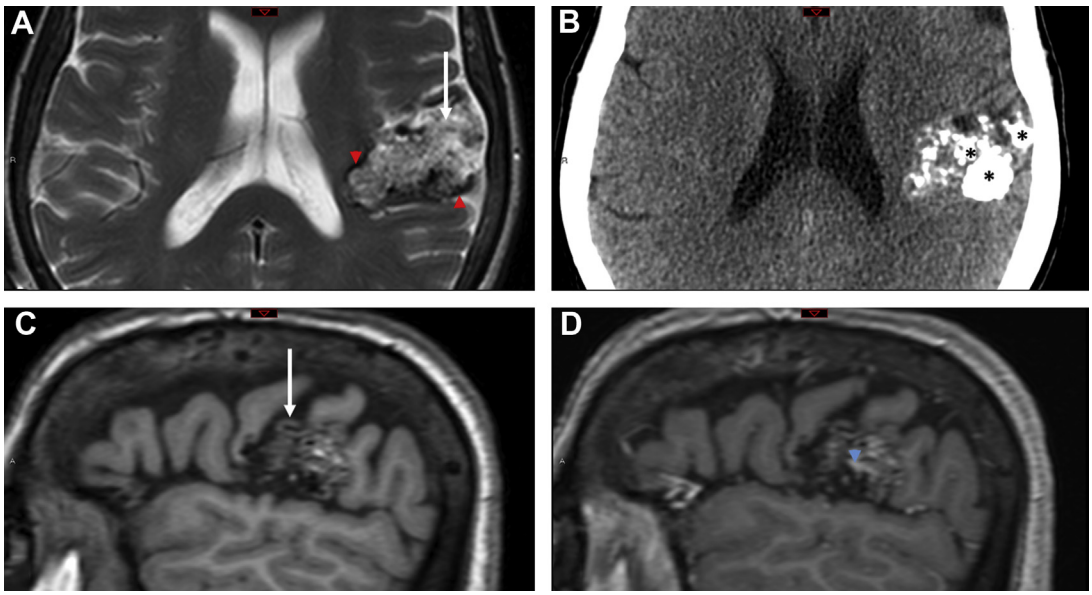


**Fig. 8.** Giant CCM. Axial T2-weighted MR image, axial noncontrast CT, and sagittal precontrast and postcontrast T1-weighted MR images in a 66 year old with focal epilepsy. The giant CCM demonstrates markedly heterogeneous hypointense/hyperintense signal on T2 and T1 images (*white arrows* in *A* and *C*, respectively) with surrounding chronic hemosiderin deposition noted as linear low T2 signal (*red arrowheads* in *A*). Faint contrast enhancement is present at the posterior lesion margin (*blue arrowhead* in *D*). The large intralesional calcific foci present in this case (*asterisks* in *B*) may be more dense and conspicuous than in other cases.

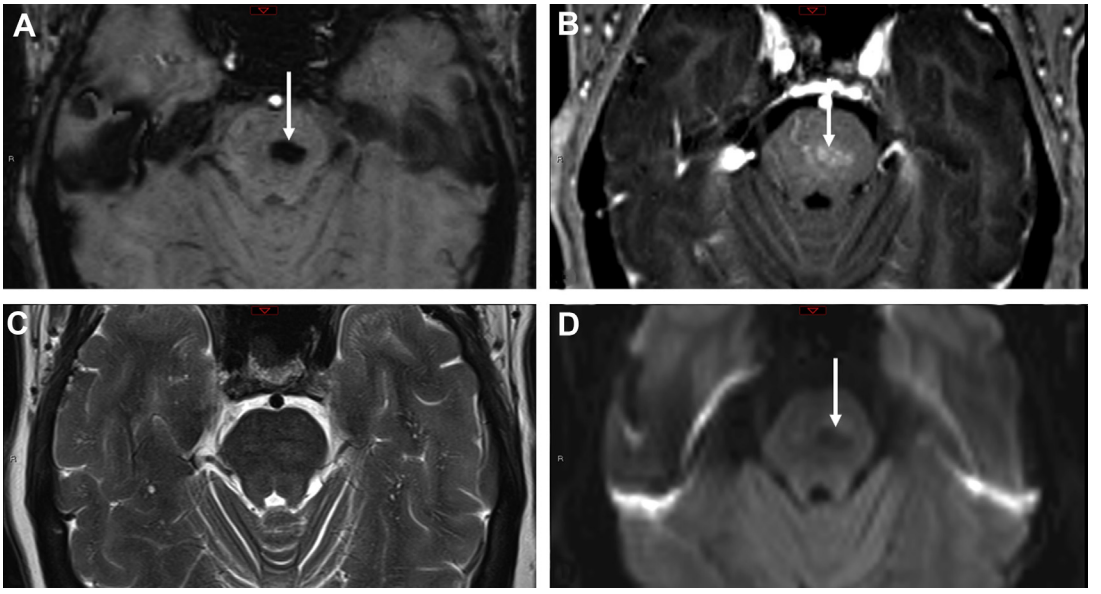


**Fig. 9.** Capillary telangiectasia. Axial SWI (*A*), axial postcontrast T1-weighted (*B*), axial T2-weighted (*C*), and axial DWI (*D*) MR images in a 72-year-old patient with lung carcinoma undergoing cerebral metastasis screening. The central pontine capillary telangiectasia is most conspicuous as a low signal intensity focus on SWI (*arrow* in *A*) with corresponding amorphous faint contrast enhancement (*arrow* in *B*). The capillary telangiectasia is nearly imperceptible on T2-weighted images and demonstrates T2 blackout effect (low signal intensity) on DWI series (*arrow* in *D*).

and mass effect, and an associated branching vein are helpful clues to the diagnosis. Stability on follow-up imaging helps confirm the diagnosis.

### *Cerebral amyloid angiopathy*

Cerebral amyloid angiopathy (CAA) results from abnormal accumulation of amyloid-β protein in cerebral cortical and leptomeningeal vessels, which predisposes to vessel rupture and hemorrhage, typically in a lobar distribution. CAA is most commonly sporadic and occurs in elderly patients. The most important neuroimaging features are sequela of prior lobar hemorrhage, including cortical/subcortical microhemorrhages and superficial siderosis, with relative sparing of the deep gray nuclei and pons. Hemorrhages are best visualized with SWI.[45] Most patients with CAA also exhibit changes of small vessel ischemia on T2-weighted imaging.

Manifestations of CAA that can mimic neoplasms are CAA-related inflammation and cerebral amyloidoma. Patients with CAA-related inflammation present with headache, rapid cognitive decline, seizure, and focal neurologic deficits. CAA-related inflammation shows large confluent regions of white matter edema with leptomeningeal contrast enhancement and local mass effect. This disease can often be identified by appreciating coexistent lobar microhemorrhages on hemosiderin-sensitive sequences (**Fig. 10**). Cerebral amyloidoma is a rare mass-like lesion that occurs in middle age patients. On imaging, it appears as a solidly enhancing white matter mass with local edema, which is difficult to prospectively distinguish from neoplasm.[46]

## LABORATORY TEST PEARLS AND PITFALLS

When confronted by imaging with a brain tumor mimic, the clinical history is crucial to guide the need for laboratory studies that may help in the diagnosis. For instance, imaging characteristics in the context of a history of immunosuppression or epidemiologic exposure raises the suspicion of an infectious cause. Thus, a detailed medical history increases the utility of ordering serologic and CSF tests. Unfortunately, for most circumstances there are no studies that determine the sensitivity and specificity of integrating the imaging characteristics and laboratory studies for a diagnosis. A pitfall of serologic diagnosis of CNS infections is the variability in sensitivity and specificity of assays and delayed antibody response after symptom onset.[47]

When a brain-enhancing lesion appears in an immunosuppressed patient, the differential diagnosis is usually between toxoplasmosis and lymphoma. Most patients with cerebral toxoplasmosis

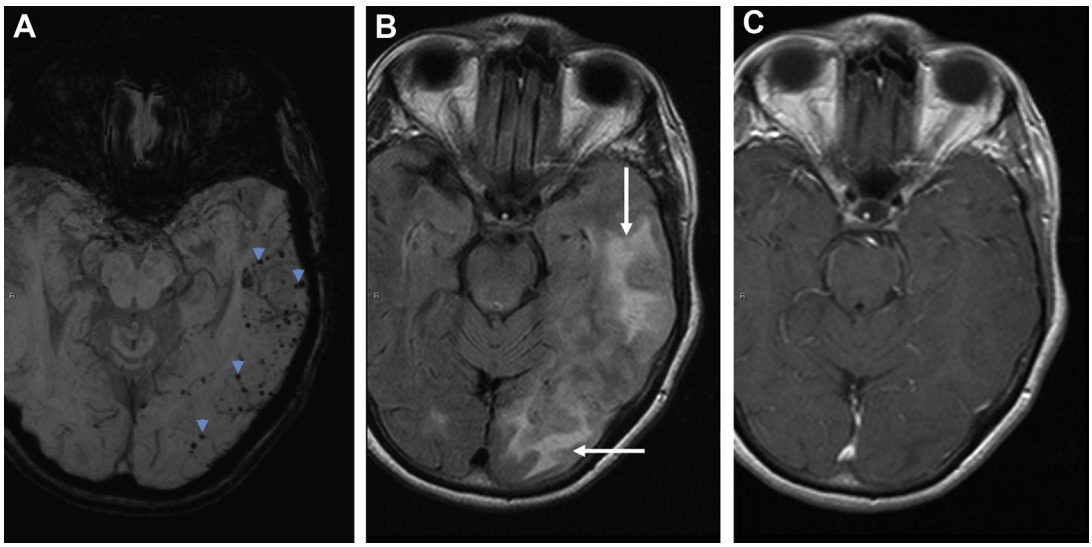


**Fig. 10.** CAA-related inflammation. Axial SWI (*A*), axial FLAIR (*B*), and axial postcontrast T1-weighted (*C*) MR images in a 66 year old with altered mental status. SWI demonstrates numerous parenchymal microhemorrhages as low signal intensity foci in a peripheral lobar distribution (*blue arrowheads* in *A*), which corresponds to the large area of temporo-occipital vasogenic edema noted on FLAIR images (*white arrows* in *B*). Minimal if any regional leptomeningeal enhancement is present on postcontrast imaging.

have high titers of antibodies against *T gondii* in blood, but a negative serologic result does not exclude the diagnosis.[48] If able to perform a lumbar puncture without risk of herniation, doing polymerase chain reaction in the CSF for *Toxoplasma* and Epstein-Barr virus may help in the diagnosis without need for a biopsy.[49] Although the specificity of CSF *Toxoplasma* polymerase chain reaction is 100%, the sensitivity is approximately 86%.[50] Therefore, a negative polymerase chain reaction does not rule out the diagnosis of CNS toxoplasmosis.

Neurocysticercosis will be in the differential diagnosis, when a brain tumor mimic is seen in an individual coming from or living in an endemic area, but there are rare cases without a clear exposure history to *T solium*. The utility of immunologic testing varies depending if the neurocysticercosis is parenchymal, extraparenchymal, or both, and the stage of the disease (viable, degenerating, or nonviable). The complement fixation test and the enzyme-linked immunosorbent assay have poor sensitivity and specificity.[51] The enzyme-linked immunoelectrotransfer blot assay in serum, which has a higher sensitivity than in CSF, is the preferred immunologic diagnostic method. Its sensitivity, however, varies from very high when there are multiple parenchymal and extraparenchymal lesions to low when there is a single parenchymal calcified lesion. Another caveat is that there may be false-positive results because of prior infection with the parasite, but without neurocysticercosis.

In the absence of systemic involvement, the diagnosis of neurosarcoidosis may be challenging. Determination of angiotensin-converting enzyme concentration is a valuable biomarker for systemic sarcoidosis. Both serum and CSF angiotensin-converting enzyme concentration, however, carry low sensitivity and specificity in neurosarcoidosis and have no predictive value in the differential diagnosis of a brain tumor mimic on MR imaging.[52]

When clinically isolated syndrome is the initial presentation of multiple sclerosis, the presence of IgG oligoclonal bands in CSF may support the diagnosis. Qualitative analysis using isoelectric focusing with immunofixation in CSF and parallel serum is the recommended methodology.[53] In two studies with long-term follow-up of patients with isolated tumefactive lesions, CSF oligoclonal bands were present in about half of the cases.[54,55] Therefore, the sensitivity for patients with multiple sclerosis presenting with a tumefactive lesion seems to be low, whereas the specificity is unknown. The anti-MOG antibody should be requested in all patients with ADEM or atypical demyelinating disease because it is a marker that in addition to imaging finding may help establish the diagnosis of MOG-associated antibody disease. The presence of anti-aquaporin-4 antibody in blood is a specific biomarker for NMOSD in the appropriate clinical and imaging settings.

## SUMMARY

Prospective identification of brain tumor mimics is an opportunity for the interpreting radiologist to add value to patient care by decreasing time to diagnosis and avoiding unnecessary surgical procedures and medical therapies, but requires familiarity with mimic entities and an appropriately high degree of suspicion.

## CLINICS CARE POINTS

- Tumor mimics may account for 4% to 13% of referrals to a neuro-oncology service, so consideration of nonneoplastic processes is critical during initial evaluation of CNS neoplasia.
- Leveraging specific imaging signs and advanced imaging techniques detailed herein may add diagnostic confidence when considering various autoimmune, infectious, and vascular tumor mimics.
- Variability in ancillary laboratory diagnostics, including serologic and various immunohistochemical tests, may confer sufficiently low negative predictive values such that tumor mimics may still be considered on a clinical and imaging basis despite an unrevealing laboratory evaluation.

## DISCLOSURE

The authors have nothing to disclose.

## REFERENCES

1. Go JL, Acharya J, Rajamohan AG. Is it or is it not? Brain tumor mimics. Semin Roentgenol 2018;53(1):62–76.
2. Leclercq D, Trunet S, Bertrand A, et al. Cerebral tumor or pseudotumor? Diagn Interv Imaging 2014;95(10):906–16.
3. Bradley D, Rees J. Brain tumour mimics and chameleons. Pract Neurol 2013;359–71. https://doi.org/10.1136/practneurol-2013-000652.
4. Starkey J, Li Y, Tihan T, et al. Clinical series: five simple MR imaging features to identify tumor mimics. Neurographics 2016;6(4):229–36.
5. Maldonado MD, Batchala P, Ornan D, et al. Features of diffuse gliomas that are misdiagnosed on initial neuroimaging: a case control study. J Neurooncol 2018;140(1):107–13.
6. Bos D, Poels MMF, Adams HHH, et al. Prevalence, clinical management, and natural course of incidental findings on brain MR images: the population-based Rotterdam Scan Study. Radiology 2016;281(2):507–15.
7. Morris Z, Whiteley WN, Longstreth WT Jr, et al. Incidental findings on brain magnetic resonance imaging: systematic review and meta-analysis. BMJ 2009;339:b3016.
8. Niessen WJ, Breteler MMB, Van Der Lugt A. Incidental findings on brain MRI in the general population. N Engl J Med 2007;357:1821–8.
9. Sarbu N, Shih RY, Jones RV, et al. White matter diseases with radiologic-pathologic correlation. Radiographics 2016;36(5):1426–47.
10. Kim E. Distinguishing tumefactive demyelinating lesions from glioma or central nervous system lymphoma: added value of unenhanced CT. Radiology 2009;251(2):467–75.
11. Given CA 2nd, Stevens BS, Lee C. The MRI appearance of tumefactive demyelinating lesions. AJR Am J Roentgenol 2004;182(1):195–9.
12. Suh CH, Kim HS, Jung SC, et al. MRI findings in tumefactive demyelinating lesions: a systematic review and meta-analysis. AJNR Am J Neuroradiol 2018;39(9):1643–9.
13. Khurana DS, Melvin JJ, Kothare SV, et al. Acute disseminated encephalomyelitis in children: discordant neurologic and neuroimaging abnormalities and response to plasmapheresis. Pediatrics 2005;116(2):431–6.
14. Kao H-W, Alexandru D, Kim R, et al. Value of susceptibility-weighted imaging in acute hemorrhagic leukoencephalitis. J Clin Neurosci 2012;19(12):1740–1.
15. Wingerchuk DM, Banwell B, Bennett JL, et al. International consensus diagnostic criteria for neuromyelitis optica spectrum disorders. Neurology 2015;85(2):177–89.
16. Shu Y, Long Y, Wang S, et al. Brain histopathological study and prognosis in MOG antibody-associated demyelinating pseudotumor. Ann Clin Transl Neurol 2019;6(2):392–6.
17. Starshinova AA, Malkova AM, Basantsova NY, et al. Sarcoidosis as an autoimmune disease. Front Immunol 2019;10:2933.
18. Bathla G, Singh AK, Policeni B, et al. Imaging of neurosarcoidosis: common, uncommon, and rare. Clin Radiol 2016;71(1):96–106.
19. Smith JK, Matheus MG, Castillo M. Imaging manifestations of neurosarcoidosis. AJR Am J Roentgenol 2004;182(2):289–95.
20. Kelley BP, Patel SC, Marin HL, et al. Autoimmune encephalitis: pathophysiology and imaging review of an overlooked diagnosis. AJNR Am J Neuroradiol 2017;38(6):1070–8.
21. Richards A, van den Maagdenberg AMJM, Jen JC, et al. C-terminal truncations in human 3'-5' DNA exonuclease TREX1 cause autosomal dominant retinal vasculopathy with cerebral leukodystrophy. Nat Genet 2007;39(9):1068–70.

22. Mateen FJ, Krecke K, Younge BR, et al. Evolution of a tumor-like lesion in cerebroretinal vasculopathy and TREX1 mutation. Neurology 2010;75(13):1211–3.
23. Schwartz KM, Erickson BJ, Lucchinetti C. Pattern of T2 hypointensity associated with ring-enhancing brain lesions can help to differentiate pathology. Neuroradiology 2006;48(3):143–9.
24. Kim JE, Kim DG, Paek SH, et al. Stereotactic biopsy for intracranial lesions: reliability and its impact on the planning of treatment. Acta Neurochir (Wien) 2003;145(7):547–55.
25. Toh CH, Wei K-C, Chang C-N, et al. Differentiation of pyogenic brain abscesses from necrotic glioblastomas with use of susceptibility-weighted imaging. AJNR Am J Neuroradiol 2012;33(8):1534–8.
26. Xu X-X, Li B, Yang H-F, et al. Can diffusion-weighted imaging be used to differentiate brain abscess from other ring-enhancing brain lesions? A meta-analysis. Clin Radiol 2014;69(9):909–15.
27. Reddy JS, Mishra AM, Behari S, et al. The role of diffusion-weighted imaging in the differential diagnosis of intracranial cystic mass lesions: a report of 147 lesions. Surg Neurol 2006;66(3):246–50.
28. Kim JH, Park SP, Moon BG, et al. Brain abscess showing a lack of restricted diffusion and successfully treated with linezolid. Brain Tumor Res Treat 2018;6(2):92–6.
29. Mahadevan A, Ramalingaiah AH, Parthasarathy S, et al. Neuropathological correlate of the "concentric target sign" in MRI of HIV-associated cerebral toxoplasmosis. J Magn Reson Imaging 2013;38(2):488–95.
30. Dibble EH, Boxerman JL, Baird GL, et al. Toxoplasmosis versus lymphoma: cerebral lesion characterization using DSC-MRI revisited. Clin Neurol Neurosurg 2017;152:84–9.
31. Floriano VH, Torres US, Spotti AR, et al. The role of dynamic susceptibility contrast-enhanced perfusion MR imaging in differentiating between infectious and neoplastic focal brain lesions: results from a cohort of 100 consecutive patients. PLoS One 2013;8(12):e81509.
32. Camacho DLA, Smith JK, Castillo M. Differentiation of toxoplasmosis and lymphoma in AIDS patients by using apparent diffusion coefficients. AJNR Am J Neuroradiol 2003;24(4):633–7.
33. Yang M, Sun J, Bai HX, et al. Diagnostic accuracy of SPECT, PET, and MRS for primary central nervous system lymphoma in HIV patients. Medicine (Baltimore) 2017;96(19):1–6.
34. Kulcsár Z, Ugron Á, Marosfoi M, et al. Hemodynamics of cerebral aneurysm initiation: the role of wall shear stress and spatial wall shear stress gradient. AJNR Am J Neuroradiol 2011;32(3):587–94.
35. Martin AJ, Hetts SW, Dillon WP, et al. MR imaging of partially thrombosed cerebral aneurysms: characteristics and evolution. AJNR Am J Neuroradiol 2011;32(2):346–51.
36. Liu JK, Gottfried ON, Amini A, et al. Aneurysms of the petrous internal carotid artery: anatomy, origins, and treatment. Neurosurg Focus 2004;17(5):1–9.
37. De Jesús O, Rifkinson N. Magnetic resonance angiography of giant aneurysms. Pitfalls and surgical implications. P R Health Sci J 1997;16(2):131–5.
38. Lev MH. Perfusion imaging of acute stroke: its role in current and future clinical practice. Radiology 2013;266(1):22–7.
39. Mathews P, Barker PB, Chatham JC, et al. Cerebral metabolites in patients with acute and subacute strokes: by quantitative proton. AJR Am J Roentgenol 1995;165:633–8.
40. Gaskill-shipley MF. Imaging of cerebral venous thrombosis: current techniques, spectrum of findings, and diagnostic pitfalls. RadioGraphics 2006;26(suppl_1):19–42.
41. Chang Y, Porbandarwala N, Rojas R. Unilateral nonvisualization of a transverse dural sinus on phase-contrast MRV: frequency and differentiation from sinus thrombosis on noncontrast MRI. AJNR Am J Neuroradiol 2019;41(1):115–21.
42. Brunereau L, Labauge P, Tournier-Lasserve E, et al. Familial form of intracranial cavernous angioma: MR imaging findings in 51 families. French Society of Neurosurgery. Radiology 2000;214(1):209–16.
43. Wang KY, Idowu OR, Lin DDM. Chapter 24 - Radiology and imaging for cavernous malformations. In: Spetzler RF, Moon K, Almefty RO, editors. Handbook of clinical neurology, vol. 143. The Netherlands: Elsevier; 2017. p. 249–66. https://doi.org/10.1016/B978-0-444-63640-9.00024-2.
44. Castillo M, Morrison T, Shaw JA, et al. MR imaging and histologic features of capillary telangiectasia of the basal ganglia. AJNR Am J Neuroradiol 2001;22(8):1553–5. Available at: http://www.ajnr.org/content/22/8/1553.abstract.
45. Haacke EM, DelProposto ZS, Chaturvedi S, et al. Imaging cerebral amyloid angiopathy with susceptibility-weighted imaging. AJNR Am J Neuroradiol 2007;28(2):316–7. Available at: http://www.ajnr.org/content/28/2/316.abstract.
46. Miller-Thomas MM, Sipe AL, Benzinger TLS, et al. Multimodality review of amyloid-related diseases of the central nervous system. RadioGraphics 2016;36(4):1147–63.
47. He T, Kaplan S, Kamboj M, et al. Laboratory diagnosis of central nervous system infection. Curr Infect Dis Rep 2016;18(11):35.
48. Colombo FA, Vidal JE, Penalva de Oliveira AC, et al. Diagnosis of cerebral toxoplasmosis in AIDS patients in Brazil: importance of molecular and immunological methods using peripheral blood samples. J Clin Microbiol 2005;43(10):5044–7.

49. Antinori A, Ammassari A, De Luca A, et al. Diagnosis of AIDS-related focal brain lesions: a decision-making analysis based on clinical and neuroradiologic characteristics combined with polymerase chain reaction assays in CSF. Neurology 1997;48(3):687–94.
50. Anselmo LMP, Vilar FC, Lima JE, et al. Usefulness and limitations of polymerase chain reaction in the etiologic diagnosis of neurotoxoplasmosis in immunocompromised patients. J Neurol Sci 2014;346(1–2):231–4.
51. Del Brutto OH. Neurocysticercosis. Handb Clin Neurol 2014;121:1445–59.
52. Bridel C, Courvoisier DS, Vuilleumier N, et al. Cerebrospinal fluid angiotensin-converting enzyme for diagnosis of neurosarcoidosis. J Neuroimmunol 2015;285:1–3.
53. Freedman MS, Thompson EJ, Deisenhammer F, et al. Recommended standard of cerebrospinal fluid analysis in the diagnosis of multiple sclerosis: a consensus statement. Arch Neurol 2005;62(6):865–70.
54. Altintas A, Petek B, Isik N, et al. Clinical and radiological characteristics of tumefactive demyelinating lesions: follow-up study. Mult Scler 2012;18(10):1448–53.
55. Siri A, Carra-Dalliere C, Ayrignac X, et al. Isolated tumefactive demyelinating lesions: diagnosis and long-term evolution of 16 patients in a multicentric study. J Neurol 2015;262(7):1637–45.